J Polym Res (2015) 22: 173
DOI 10.1007/s10965-015-0813-4

ORIGINAL PAPER

A novel surface modification for calcium sulfate whisker used for reinforcement of poly(vinyl chloride)

Wenjin Yuan[1] · **Jiayang Cui**[1] · **Yangben Cai**[1] · **Shiai Xu**[1,2]

Received: 28 March 2015 / Accepted: 23 July 2015 / Published online: 12 August 2015

Abstract A novel technique is developed in this study to modify the surface of calcium sulfate whisker (CSW) for the preparation of high-performance CSW/poly(vinyl chloride) (PVC) composites. The CSW coated with poly(vinyl alcohol) (PVA) and then cross-linked by glutaraldehyde is used to strengthen PVC, and the surface morphology and mechanical properties of CSW/PVC composites are investigated. It shows that the mechanical properties of the cross-linked PVA modified CSW/PVC (cPVA@CSW/PVC) composites are significantly improved, their yield strength, breaking strength, tensile modulus and elongation at break are 65.7 MPa, 53.5 MPa, 1772 MPa and 225 %, with an increase of 7.2, 13.1, 7.6 and 8.2 % as compared with that of the unmodified CSW/PVC composites, respectively. The improvement in the mechanical properties can be attributed to the strong interfacial adhesion between cPVA@CSW and PVC matrix, because the modified CSW has abundant hydroxyl groups that can produce a strong interaction with PVC. This method is simple and inexpensive, and can be applied in large scale.

Keywords Poly(vinyl chloride) composites · Calcium sulfate whisker · Cross-linked poly(vinyl alcohol) · Morphology · Mechanical properties

✉ Shiai Xu
saxu@ecust.edu.cn

[1] Shanghai Key Laboratory of Advanced Polymeric Materials, Key Laboratory for Ultrafine Materials of Ministry of Education, School of Materials Science and Engineering, East China University of Science and Technology, Shanghai 200237, China

[2] The Chemical Engineering College of Qinghai University, Xining 810016, China

Introduction

Calcium sulfate whisker (CSW) is a kind of fiber-shaped single crystal with many advantageous properties, such as large length-to-diameter ratio, high strength and stiffness, good thermal stability, and few internal defects such as dislocations [1], which make it a preferred filler over many conventional fillers, such as calcium carbonate and natural fiber. Another particular advantage of CSW is its lower price than the other high performance fillers, such as carbon nanotubes and graphene. Therefore, CSW has gained increasing interest due to its potential applications in a myriad of polymer composites [2].

Extensive studies have been conducted on the preparation of organic CSW. Wang et al. [1] have successfully prepared a series of CSWs using carbide slag as raw material by the hydrothermal method. The prepared gypsum was hemihydrate calcium sulfate and the formation of CSWs was influenced by the preparation conditions. Lü et al. [3] investigated the effect of calcium monohydrogen phosphate on the morphology of CSW prepared by hydrothermal synthesis. CSWs were mainly applied to strengthen polypropylene (PP) [4], PA-66 [5], and non-metallic friction materials such as phenolic resin [6].

There are many difficulties in preparing high-performance CSW/polymer composites. For instance, challenges remain to guarantee a homogeneous dispersion of whiskers in the polymer matrix [7], and a good interfacial interaction between the whiskers and the surrounding matrix [8–10]. The incompatibility results in a poor load transfer between the hydrophilic whiskers and the hydrophobic polymer matrix, and thus the whiskers can be easily pulled out from the polymer matrix, resulting in a limited reinforcement. A variety of physical methods, such as solution blending [11] and high shear mixing [12], and chemical methods, such as covalent [13] and non-covalent [14] modification of the filler surface, have been used

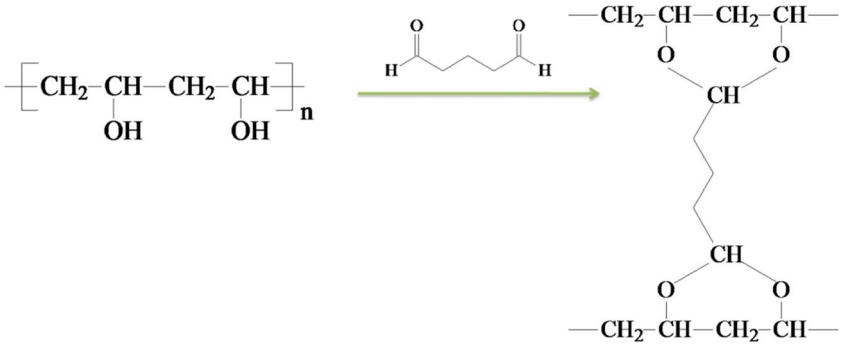

Fig. 1 The cross-linking mechanism of PVA

to improve the dispersion of the fillers in the polymer matrices and the interfacial interaction [15]. However, most of these methods are either of low efficiency, especially for the physical methods, or quite inconvenient (e.g., grafting [16] and using coupling agent [17]) during the modification process. This highlights the need for a more efficient and simple method to modify the whisker surface for the preparation of high-performance whisker/polymer composites.

Poly(vinyl chloride) (PVC) is an important polymer with versatile physical-chemical (e.g., easy fabrication and long lasting) and biological properties. Many polymer composites have been prepared using PVC as the matrix and natural fibers (e.g., wood [18], rice hull [19] and kenaf [20]), nanoparticles [21, 22], graphene [23, 24], and whiskers (e.g., potassium titanate whiskers [25] and cellulose whiskers [26]) as the fillers. However, to the best of our knowledge, CSW has rarely been used to reinforce PVC.

In this study, a simple yet effective method was proposed for the preparation of CSW/PVC composites with excellent mechanical and thermal properties. This method is based on the cross-linking reaction of PVA to cladding to the whisker surface. The hydrophilic PVA can easily spread out on the whisker surface and be tightly bonded to CSW after cross-linking reaction, and the polar functional group of the acetalized PVA has a strong interaction with the polar PVC, resulting in a significant improvement in the compatibility between cPVA@CSW and PVC. The resultant cPVA@CSW/PVC composites show better strength, stiffness, elongation at break, dynamic mechanical and thermal properties than the unmodified CSW. The effect of the dispersion and interfacial interaction of CSW on the performance is also investigated.

Experimental

Materials

PVC (SG-5) was purchased from Dongguan Dansheng Plastic Materials Co., Ltd. (Dongguan, China); CSW was purchased

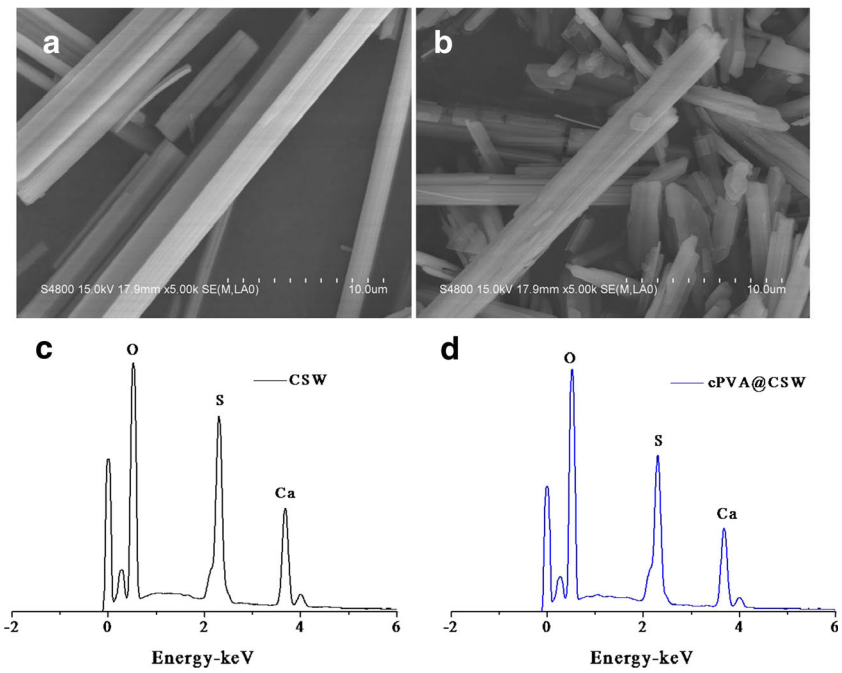

Fig. 2 Surface morphology and EDS spectra of uncoated CSW (**a** and **c**) and cPVA@CSW (**b** and **d**)

Table 1 The EDS results of CSW and cPVA@CSW

Sample	CSW		cPVA@CSW	
	Weight (wt.%)	Atom (at.%)	Weight (wt.%)	Atom (at.%)
O	42.9±2.6	62.9±2.4	48.5±2.1	68.0±1.9
Ca	33.0±1.1	19.4±1.0	29.8±0.7	16.7±0.7
S	24.1±1.5	17.7±1.4	21.7±1.4	15.3±1.2

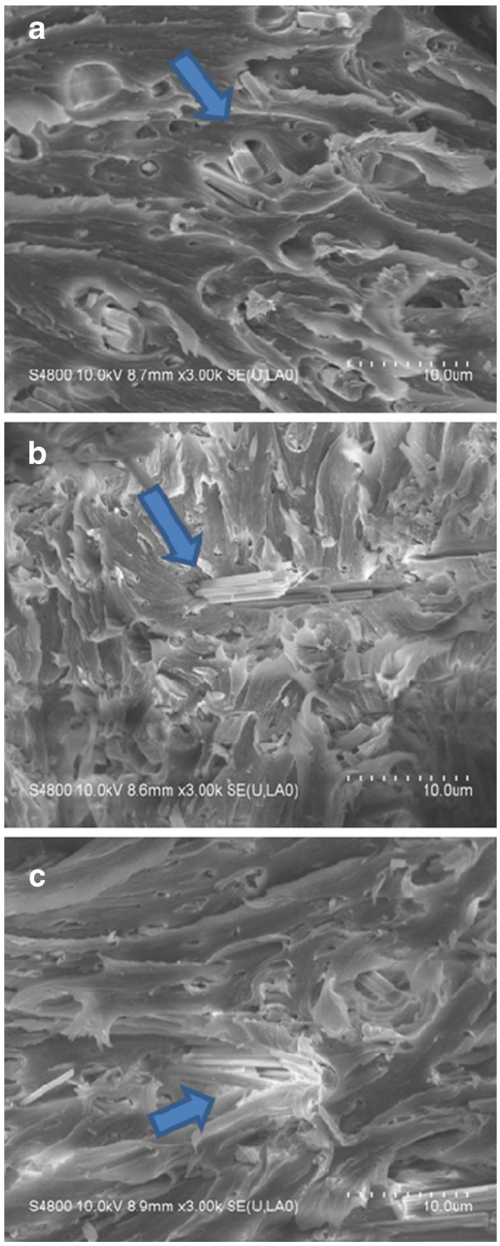

Fig. 3 SEM images of tensile fracture surfaces of **a** CSW/PVC (5 wt.% whisker), **b** 0.1 % cPVA@CSW /PVC (5 wt.% whisker), and **c** 1 % cPVA@CSW /PVC (5 wt.%whisker)

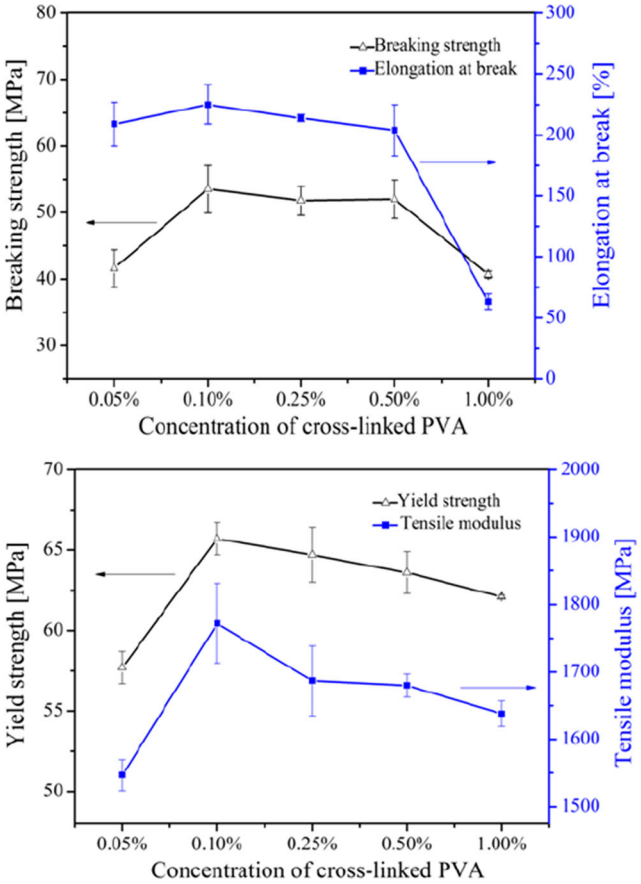

Fig. 4 Effects of concentration of cross-linked PVA on mechanical properties of cPVA@CSW/ PVC

from Shanghai Fengzhu Trading Co., Ltd (Shanghai, China); Organic tin, dioctyl phthalate (DOP), glyceryl monosterate (GMS), acrylic processing aid (ACR) and paraffin wax were commercially available, all of them were of technical grade; and PVA (PVA1750) and glutaraldehyde solution were purchased from Sinopharm Chemical Reagent Co., Ltd. (Shanghai, China).

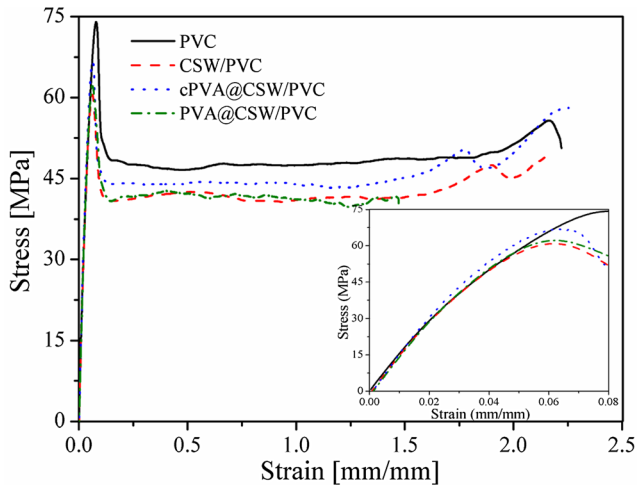

Fig. 5 Typical stress–strain curves for PVC and its composites

Table 2 Mechanical properties of the composites

Sample	Yield strength (MPa)	Breaking strength (MPa)	Tensile modulus (MPa)	Elongation at break (%)
Pristine PVC	67.9±1.6	44.6±1.0	1551±33	214±6
CSW/PVC	61.3±1.5	47.3±3.4	1647±39	208±13
PVA@CSW/PVC	62.6±0.2	42.3±1.9	1654±25	158±42
cPVA@CSW/PVC	65.7±1.0	53.5±3.6	1772±59	225±16

Preparation

Preparation of cross-linked PVA coated CSW (cPVA@CSW)

cPVA@CSWs were prepared as follows: 1 g of 1 wt.% PVA aqueous solution, 30 mL of deionized water and 10 g of dried CSW were added sequentially into a 100 mL three-necked round-bottom flask fitted with a mechanical overhead stirrer. Then, 1 drop of 25 % glutaraldehyde solution and 5 drops of 0.5 mol/L sulfuric acid solution were added, which served as the cross-linking agent and pH adjuster, respectively. The mixture was stirred at room temperature for 1 h, and the obtained products were dried under vacuum at 80 °C for 2 h to complete the cross-linking reaction and remove excess water. The cross-linking mechanism was outlined in Fig. 1. Different amounts of 1 wt.% PVA aqueous solution were applied to modify CSW to investigate their effects on the mechanical properties of cPVA@CSW.

Preparation of CSW/PVC and cPVA@CSW/PVC composites

PVC resin (100 phr) was mixed with CSW (5 phr), using organic tin (2 phr) as the heat stabilizer and DOP (4 phr) as the plasticizer. GMS (0.6 phr), ACR (4 phr) and paraffin wax (0.4 phr) were then added. All PVC constitutes were mixed uniformly and processed using a two-roll mill at 170 °C. The resultant compound was molded into rectangular sheets by compression molding at 170 °C and 10 MPa for 5 min using a plate vulcanizing press.

The cPVA@CSW/PVC composites were prepared by the same procedures.

Characterization

Scanning electron microscopy

The whisker surface and fracture surface of the tensile samples, coated with a thin gold layer before testing, were characterized by scanning electron microscopy (SEM, S-4800, Hitachi), and the element content on the surface of CSW was calculated using an EDS system (QUANTAX 400–30).

Tensile testing

The mechanical properties were determined using a MTS E44 universal testing machine in accordance with ISO 527, and the average values and standard deviations were derived from at least five independent tests for each sample.

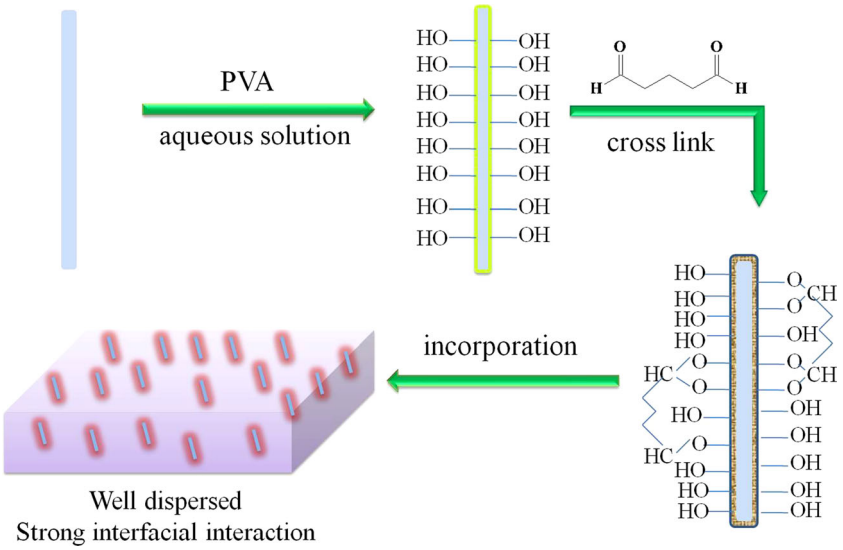

Fig. 6 The interfacial interaction between the cross-linked PVA and the CSW/PVC composites

Dynamic mechanical analysis

The dynamic properties of the composites were determined using dynamic mechanical analysis (DMA) on a TA Instruments Q800 in a three-point bending mode. The specimens were heated from 25 to 140 °C at a heating rate of 3 °C/min and then tested at a vibration frequency of 1 Hz.

Thermogravimetric analysis

Thermogravimetric analysis (TGA) was carried out at a heating rate of 10 °C/min to 600 °C under a nitrogen atmosphere using a Netzsch STA 409PC thermogravimetric analyzer.

Results and discussion

Interfacial morphology

Figure 2a and b show the SEM images of CSW and cPVA@CSW, and Fig. 2c and d show their corresponding EDS spectra, respectively. It is clear that the uncoated CSW has a smooth surface (Fig. 2a), and is composed of O (42.9 wt.%), Ca (33.0 wt.%) and S (24.1 wt.%) (Fig. 2c and Table 1), which is approximately consistent with the formula of $CaSO_4$. The surface of cPVA@CSW is coarse, indicating that a thin film is coated on the surface of cPVA@CSW (Fig. 2b). The diameter of the whisker decreases after modification, because cross-linked PVA coated on CSW can prevent the agglomeration of CSW. The modified whisker is composed of O (48.5 wt.%), Ca (29.8 wt.%) and S (21.7 wt.%) (Fig. 2d and Table 1). The formation of the organic layer results in an increase in the content of O and a decrease in the contents of Ca and S.

Figure 3 shows the SEM images of the fracture surface of tensile specimens, where the content of whisker in all composites is 5 wt.%. In untreated CSW/PVC composite, some whisker pullouts and gaps between whiskers and matrix are observed, as indicated by the arrow. Moreover, the edges and ends of the untreated CSW in the composite are very smooth (Fig. 3a). cPVA@CSW hybrid seems to be sticky with the PVC matrix and the interface is rough and adhesive (Fig. 3b). The enhanced interfacial interaction between the CSW and the polymeric matrix should be due to the coating of cross-linked PVA. The hydrophobic polymer does not wet or interact with the hydrophilic fillers because of the differences in surface energy [27]. For the cPVA@CSW/PVC composites, the abundant hydroxyl and ether groups formed on the surface of modified whiskers during the cross-linking process have a strong electrostatic interaction with the PVC matrix, thus leading to excellent compatibility and interfacial adhesion between whiskers and PVC [28].

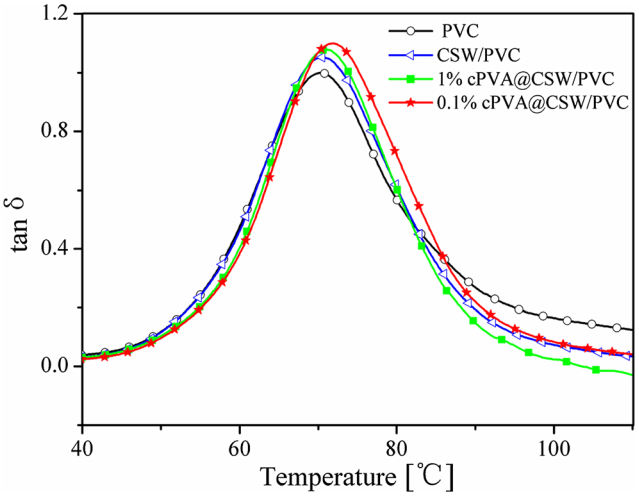

Fig. 7 Loss tangent (tanδ) as a function of temperature for PVC and its composites at a constant frequency of 1 Hz

Figure 3b and c show the effect of the concentration of cross-linked PVA on the morphology of the composites. As the PVA concentration increases, the whiskers tend to stick to each other, which leads to the formation of agglomerates and finally impacts the performance of the composites. This may be ascribed to the cohesiveness of PVA which will bond whiskers together after exceeding a certain threshold level, leading to the poor performance of the composites.

Mechanical performance

Figure 4 shows the effect of the concentration of cross-linked PVA on the mechanical properties of cPVA@CSW/PVC composites. It is found that the yield strength, tensile modulus, breaking strength and elongation at break of the composites increase with the increase of PVA concentration from 0.05 to 0.1 wt.% of CSWs, and then decrease with further increase of the concentration, indicating that too high or too low

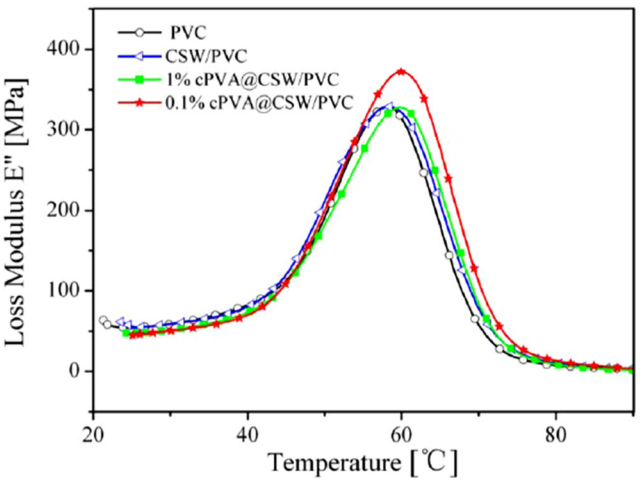

Fig. 8 Loss modulus as a function of temperature for PVC and its composites at a constant frequency of 1 Hz

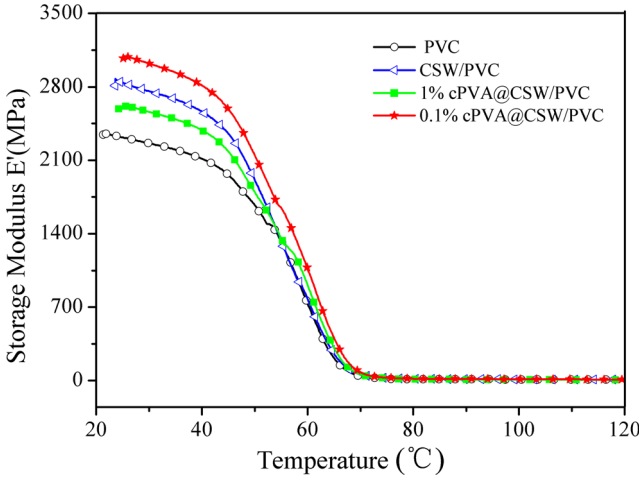

Fig. 9 Storage modulus as a function of temperature for PVC and its composites at a constant frequency of 1 Hz

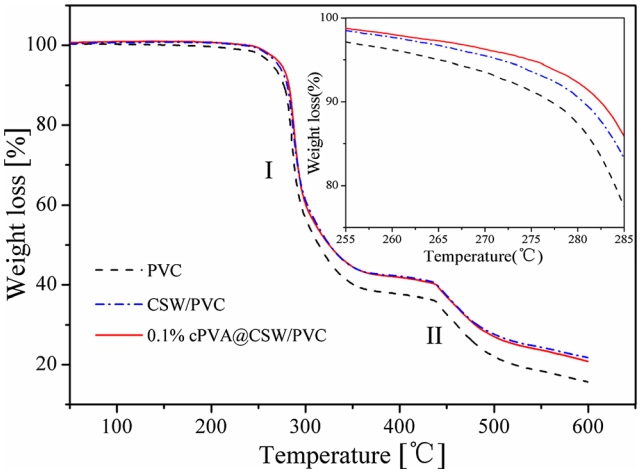

Fig. 10 TGA curves of PVC and its composites

concentration of PVA is unfavorable to the mechanical properties of the resulting cPVA@CSW/PVC composites. If the concentration of PVA is too low, PVA cannot completely coat the surface of CSWs, resulting in weak interfacial interaction between the whiskers and PVC matrix. However, too high concentration of PVA may make the whiskers stick together and result in a high stress concentration in PVC matrix, thus leading to a poor mechanical performance. This is especially true for 1 wt.% cross-linked PVA, as the elongation at break for the corresponding composite decreases significantly. It can be concluded from Fig. 4 that the optimal concentration of PVA is 0.1 wt %. D. Metin et al. [29] also showed that there was an optimal concentration of the coupling agent for the mechanical behavior of the polypropylene/natural zeolite composite. It appears that the thickness of the organic coating on the surface of inorganic filler plays a key role in improving the mechanical properties of the composites.

Figure 5 shows typical stress–strain curves for PVC and its composites, and Table 2 summarizes the mechanical properties of the samples. The mechanical properties of the composites have been improved upon coating the CSW with the cross-linked PVA, and the yield strength, breaking strength, tensile modulus and elongation at break of cPVA@CSW/PVC are 65.7 MPa, 53.5 MPa, 1772 MPa and 225 %, with an increase of 7.2, 13.1, 7.6 and 8.2 % as compared with the unmodified CSW/PVC composites, respectively. Thus, cross-linked PVA makes a significant contribution to improving the interfacial adhesion between whisker and PVC matrix. This can be attributed to the fact that the hydrophilic PVA can easily spread out on the surface of whiskers and produce strong interaction with CSW. PVA tightly encases CSWs after being cross-linked by glutaraldehyde. The polar functional groups of the acetalized PVA can form strong interaction with the polar PVC, including hydrogen bonding, which can significantly improve the interfacial strength between CSW and PVC. Figure 6 shows the interfacial interaction mechanism of the cPVA@CSW/PVC composites. The mechanical properties of uncross-linked PVA@CSW/PVC composite are also tested and compared. The yield strength of uncross-linked PVA@CSW/PVC composite is higher than that of CSW/PVC. This can be attributed to the fact that there are many hydroxyl groups on the surface of uncross-linked PVA@CSW, which can improve the interaction between whiskers and PVC matrix, and thus lead to a better mechanical behavior. However, it is lower than that of cPVA@CSW/PVC composite, because PVA tightly encases CSWs after being cross-linked by glutaraldehyde. Thus, the interfacial interaction of cPVA@CSW/PVC composite is much stronger than that of uncross-linked PVA@CSW/PVC composite, leading to a much better mechanical performance.

Dynamic mechanical properties

DMA is a reliable method used to characterize the relaxation behavior of materials. In this study, the thermomechanical properties of the PVC composites, including loss tangent (tan δ), loss modulus (E") and storage modulus (E'), were

Table 3 Glass transition temperature of PVC and its composites

Sample	Pristine PVC	CSW/PVC	1 % cPVA@CSW/PVC	0.1 % cPVA@CSW/PVC
T_g(°C)	70.3	70.4	70.7	71.6

determined by DMA, and the results are shown in Figs. 7, 8 and 9, respectively.

Table 3 shows that the glass transition temperature (T_g) of the composite hardly changes after filling with CSWs. Because of the interfacial interaction between PVC and the modified whiskers, the T_g values of cPVA@CSW/PVC composites are slightly higher than that of untreated CSW/PVC, and 0.1 % cPVA@CSW/PVC composite has the highest T_g. The similar trend is also observed in loss modulus curves (Fig. 8).

Figure 9 shows that storage modulus decreases slowly with increasing temperature in the range of <50°C and >80 °C, and more rapidly in the range of 50-80 °C, which agrees well with the relaxation behavior of polymer chains in the glass transition zone. The 0.1 % cPVA@CSW/PVC composite shows a higher storage modulus than the untreated CSW/PVC at a temperature lower than T_g, indicating that the strong interaction of cross-linked PVA coated CSWs with PVC could restrain the motion of PVC chains. Thus, the applied stress can be transferred from the matrix to the whiskers, resulting in an improvement of the mechanical properties. The 0.1 % cPVA@CSW/PVC composite also has a much higher storage modulus than the 1 % cPVA@CSW/PVC composite, indicating that PVA concentration has a significant effect on the property of the composites.

It is interesting to note that modified CSW exhibits different reinforcement effects at different temperature ranges. At low temperatures, 0.1 % cPVA@CSW/PVC has the highest storage modulus, while 1 % cPVA@CSW/PVC has the lowest storage modulus, indicating that a too thick PVA coating is detrimental to the modulus of the composites. However, at high temperatures, the storage modulus of 1 % cPVA@CSW/PVC composite is generally higher than that of CSW/PVC composite, and 0.1 % cPVA@CSW/PVC composite has the highest modulus. The elastic modulus and glass transition temperature of PVA are lower than those of PVC, indicating that PVA is softer than PVC below the glass transition temperature of PVC. Therefore, a thick PVA coating on the surface of CSW results in decrease in storage modulus. When the temperature increases to the glass transition zone of PVC, the matrix in rubber state becomes soft. CSWs have no reinforcement effects in this case because of the poor interfacial interaction between the whiskers and the matrix [30, 31], thus CSW/PVC composite has the lowest storage modulus.

Thermal properties

The TGA curves of pure PVC resin and its composites loaded with CSW and cPVA@CSW are shown in Fig. 10. It shows that there are two weight loss stages (I and II) for both the pristine PVC and the composites. The decomposition of pristine PVC starts at about 276 °C and ends at about 298 °C (stage I) with 61 % of weight loss, which corresponds to the dehydrochlorination (HCl evolution) [32]. At high temperatures, chlorine radicals resulting from the cleavage of -C-Cl labile bonds take off a hydrogen radical from adjacent -C-H groups to form a covalent H-Cl bond. This chemical process induces double bonds along the polymer chain and may lead to conjugated polymeric chains. From 298 to 435 °C, the sample becomes thermally stable again due to the formation of conjugated double bonds after HCl evolution. A new polymer, polyacetylene, which is more heat stable than PVC, is formed [33]. A second decomposition stage (stage II) occurs from 435 to 489 °C, which is corresponding to the polyacetylene cracking (scission of covalent and multiple bonds). Above 489 °C, a stable residue, i.e., carbon black, is formed [34].

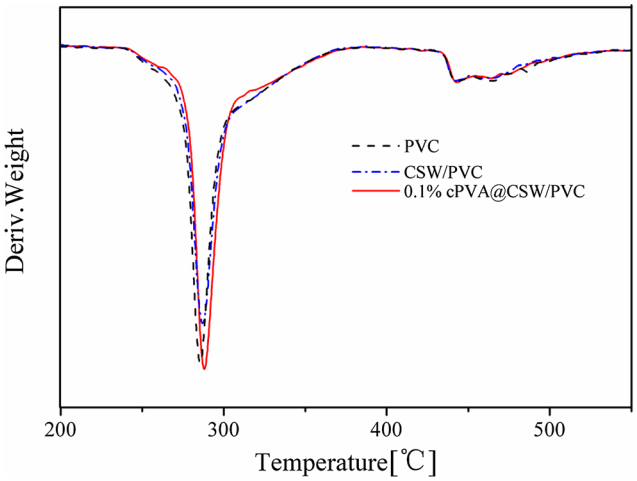

Fig. 11 DTG curves of PVC and its composites

Similar to pure PVC, the composites also show a two-stage degradation. The two peaks in the derivative thermograms (Fig. 11), indicative of the maximum weight loss rate of the degradation, correspond to the rapidest degradation temperature of each stage [35]. The temperatures of onset decomposition (T_{onset}), the rapidest decomposition (T_{rpd}) and the 50 % weight loss residue (T_{50}) are summarized in Table 4. It shows that both T_{onset} and T_{rpd} of the CSW/PVC composite are slightly increased as compared to the unfilled PVC. After modification, T_{onset} and T_{rpd} of the cPVA@CSW/PVC composite are further increased. This may be ascribed to the

Table 4 Degradation temperatures of PVC and its composites obtained from TGA and DTG curves

Sample	Temperature (°C)		
	T_{onset}	T_{rpd}	T_{50}
Pristine PVC	276	285	314
CSW/PVC	277	286	325
0.1 % cPVA@CSW/PVC	279	288	325

*The content of CSW in all composites is 5 wt. %

physical barrier effect of CSWs which can retard the decomposition of the composites and create more tortuous pathways in the PVC matrix for the penetration of volatile degradation products [36, 37]. The further increase in T_{onset} and T_{rpd} of the cPVA@CSW/PVC composite is indicative of an enhancement of the interfacial adhesion between whiskers and PVC matrix, which can improve the performance of the composites. The results of T_{50} clearly show that the presence of filler increases the thermal stability of the PVC composites [34, 38]. However, on the whole, the incorporation of CSW has no significant impact on the thermal degradation behavior of the composites.

Conclusions

CSW surface can be effectively modified by coating a layer of PVA cross-linked by glutaraldehyde, which can prevent the aggregation of CSW, and the modified CSW can be dispersed very well in the PVC matrix. There exists a strong interaction between the modified CSW and the PVC matrix, which results in a significant improvement of the mechanical properties of the composites. The optimal concentration of PVA is 0.1 wt. % relative to CSW, and too low or too high PVA concentration is detrimental to the reinforcement of CSW. The yield strength, breaking strength, tensile modulus and elongation at break of 0.1 wt.% cPVA@CSW/PVC composite are 65.7 MPa, 53.5 MPa, 1772 MPa and 225 %, with an increase of 7.2, 13.1, 7.6 and 8.2 % as compared with that of unmodified composite, respectively. The new method developed in this study is simple and effective, and is suitable for large-scale industrial applications. Another particular advantage of this method is that it needs no toxic solvent or complex grafting procedure.

Acknowledgments We gratefully acknowledge the financial support of Qinghai Science & Technology Department and the Fundamental Research Funds for the Central University.

References

1. Wang Y, Li Y, Yuan A, Yuan B, Lei X, Ma Q, Han J, Wang J, Chen J (2014) Preparation of calcium sulfate whiskers by carbide slag through hydrothermal method. Cryst Res Technol 49(10):800–807
2. Qin J, Shi W, Yang H, Liu J, Yu J, Lv Q, Tian Y (2013) Sonochemical activation calcium sulfate whisker with enhanced beta-nucleating ability for isotactic polypropylene. Colloid Polym Sci 291(11):2579–2587
3. Lü P, Fei D, Dang Y (2014) Effects of calcium monohydrogenphosphate on the morphology of calcium sulfate whisker by hydrothermal synthesis. Can J Chem Eng 92(10): 1709–1713
4. Wang XL, Zhu YM, Han YX, Yuan ZT, Yin WZ (2009) Toughening of polypropylene with calcium sulfate whiskers treated by coupling agents. Adv Mater Res 58:225–229
5. Wang H-G, Mu B, Ren J-F, Jian L-Q, Zhang J-Y, Yang S-R (2009) Mechanical and tribological behaviors of PA66/PVDF blends filled with calcium sulphate whiskers. Polym Compos 30(9):1326–1332
6. Zhu Z, Xu L, Chen G, Li Y (2010) Optimization on tribological properties of aramid fibre and CaSO4 whisker reinforced non-metallic friction material with analytic hierarchy process and preference ranking organization method for enrichment evaluations. Mater Des 31(1):551–555
7. Kim H, Miura Y, Macosko CW (2010) Graphene/Polyurethane nanocomposites for improved gas barrier and electrical conductivity. Chem Mater 22(11):3441–3450
8. Kim H, Abdala AA, Macosko CW (2010) Graphene/Polymer nanocomposites. Macromolecules 43(16):6515–6530
9. Gong L, Kinloch IA, Young RJ, Riaz I, Jalil R, Novoselov KS (2010) Interfacial stress transfer in a graphene monolayer nanocomposite. Adv Mater 22(24):2694–2697
10. Gonçalves G, Marques PAAP, Barros-Timmons A, Bdkin I, Singh MK, Emami N, Grácio J (2010) Graphene oxide modified with PMMA via ATRP as a reinforcement filler. J Mater Chem 20(44): 9927–9934
11. Ljungberg N, Cavaillé JY, Heux L (2006) Nanocomposites of isotactic polypropylene reinforced with rod-like cellulose whiskers. Polymer 47(18):6285–6292
12. Thostenson ET, Chou T-W (2006) Processing-structure-multi-functional property relationship in carbon nanotube/epoxy composites. Carbon 44(14):3022–3029
13. Sainsbury T, Erickson K, Okawa D, Zonte CS, Fréchet JMJ, Zettl A (2010) Kevlar functionalized carbon nanotubes for next-generation composites. Chem Mater 22(6):2164–2171
14. Liu J, Bibari O, Mailley P, Dijon J, Rouvière E, Sauter-Starace F, Caillat P, Vinet F, Marchand G (2009) Stable non-covalent functionalisation of multi-walled carbon nanotubes by pyrene–polyethylene glycol through π–π stacking. New J Chem 33(5):1017–1024
15. Kun Yao GZ, Lin Y, Gong J, Na H, Tang T (2015) One-pot approach to prepare high-performance graphene-reinforced poly(vinyl chloride) using lithium alkyl as covalent bonding agent. Polym Chem 6(3):389–396
16. Junior de Menezes A, Siqueira G, Curvelo AAS, Dufresne A (2009) Extrusion and characterization of functionalized cellulose whiskers reinforced polyethylene nanocomposites. Polymer 50(19):4552–4563
17. Cheng G, Qian J, Miao J, Yang B, Xia R, Chen P (2014) The surface modification of TiN nano-particles using macromolecular coupling agents, and their resulting dispersibility. Appl Surf Sci 301:79–84
18. Chaochanchaikul K (2012) Photodegradation profiles of PVC compound and wood/PVC composites under UV weathering. Express Polym Lett 7(2):146–160
19. Petchwattana N, Covavisaruch S, Pitidhammabhorn D (2013) Influences of water absorption on the properties of foamed poly(-vinyl chloride)/rice hull composites. J Polym Res 20(6):172–178
20. El-Shekeil YA, Sapuan SM, Jawaid M, Al-Shuja'a OM (2014) Influence of fiber content on mechanical, morphological and thermal properties of kenaf fibers reinforced poly(vinyl chloride)/thermoplastic polyurethane poly-blend composites. Mater Des 58:130–135
21. Zarrinkhameh M, Zendehnam A, Hosseini SM (2013) Electrochemical, morphological and antibacterial characterization of PVC based cation exchange membrane modified by zinc oxide nanoparticles. J Polym Res 20(11):283–291
22. Kong Q, Tang Y, Hu Y, Song L, Liu H, Li L (2011) Thermal stability and flame retardance properties of acrylonitrile-butadiene-styrene/polyvinyl chloride/organophilic Fe-montmorillonite nanocomposites. J Polym Res 19(1):9751–9760
23. Saadatabadi NM, Nateghi MR, Borhanizarandi M (2014) Fabrication and characterization of nanosilver intercalated

graphene embedded poly(vinyl chloride) composite thin films. J Polym Res 21(8):527–535
24. Deshmukh K, Khatake SM, Joshi GM (2013) Surface properties of graphene oxide reinforced poly(vinyl chloride) nanocomposites. J Polym Res 20(11):286–296
25. Chen LF, Hong YP, Zhang Y, Qiu JL (2000) Fabrication of polymer matrix composites reinforced with controllably oriented whiskers. J Mater Sci 35(21):5309–5312
26. Chazeau L, Paillet M, Cavaille JY (1999) Plasticized PVC reinforced with cellulose whiskers. I. Linear viscoelastic behavior analyzed through the quasi-point defect theory. J Polym Sci, Part B: Polym Phys 37(16):2151–2164
27. Ruckenstein E, Park JS (1992) Stable concentrated emulsions as precursors for hydrophilic-hydrophobic polymer composites. Polymer 33(2):405–417
28. Zhu A, Cai A, Zhou W, Shi Z (2008) Effect of flexibility of grafted polymer on the morphology and property of nanosilica/PVC composites. Appl Surf Sci 254(13):3745–3752
29. Metın D, Tihminlioğlu F, Balköse D, Ülkü S (2004) The effect of interfacial interactions on the mechanical properties of polypropylene/natural zeolite composites. Compos Part A 35(1): 23–32
30. Masaya Kawasumi NH, Kato M, Usuki A, Okada A (1997) Preparation and mechanical properties of polypropylene-clay hybrids. Macromolecules 30(20):6333–6338
31. Vadukumpully S, Paul J, Mahanta N, Valiyaveettil S (2011) Flexible conductive graphene/poly(vinyl chloride) composite thin films with high mechanical strength and thermal stability. Carbon 49(1):198–205
32. Djidjelli HST, Benachour D (2000) Effect of plasticizer nature and content on the PVC stability and dielectric properties. J Appl Polym Sci 78(3):685–691
33. Benavides RCB, Castañeda AO, López GM, Arias G (2001) Different thermo-oxidative degradation routes in poly(vinyl chloride). Polym Degrad Stab 73(3):417–423
34. Bishay IK, Abd-El-Messieh SL, Mansour SH (2011) Electrical, mechanical and thermal properties of polyvinyl chloride composites filled with aluminum powder. Mater Des 32(1):62–68
35. Gong F (2004) Thermal properties of poly(vinyl chloride)/montmorillonite nanocomposites. Polym Degrad Stab 84(2):289–294
36. Chozhan C, Alagar M, Gnanasundaram P (2009) Synthesis and characterization of 1,1-bis(3-methyl-4-hydroxy phenyl)cyclohexane polybenzoxazine–organoclay hybrid nanocomposites. Acta Mater 57(3):782–794
37. Herrera-Alonso JM, Marand E, Little J, Cox SS (2009) Polymer/clay nanocomposites as VOC barrier materials and coatings. Polymer 50(24):5744–5748
38. Li X, Lei B, Lin Z, Huang L, Tan S, Cai X (2014) The utilization of bamboo charcoal enhances wood plastic composites with excellent mechanical and thermal properties. Mater Des 53:419–424